J Electroceram (2007) 19:221–228
DOI 10.1007/s10832-007-9332-y

Crystallization and dielectric properties of borate-based ferroelectric $PbTiO_3$ glass-ceramics

Pat Sooksaen · Ian M. Reaney · Derek C. Sinclair

Received: 22 August 2006 / Accepted: 12 September 2007 / Published online: 3 October 2007

Abstract Bulk crystallized $PbTiO_3$ (PT) was the major crystalline phase in borate-based glass ceramics with starting composition $39PbO–1BaO–25TiO_2–9.8Al_2O_3–1SiO_2–24.2B_2O_3$ (mol%). Crystallization of PT starts at ≥520 °C and the crystal size and *c*/*a* ratio of PT were approximately the same for all samples heat treated between 520 and 700 °C. Two transient unidentified phases were induced when crystallized between 520 and 650 °C. The first at 520 °C followed by a second at 550 °C. At >650 °C, $PbTi_3O_7$ was present in addition to $PbTiO_3$. The electrical properties of glasses heat treated between 550–700 °C were investigated by fixed frequency capacitance measurements and impedance spectroscopy, IS. No permittivity maximum or Curie temperature, T_c, for the PT phase was observed from fixed frequency capacitance measurements for glasses heat treated below 700 °C, however IS data analysis using electric modulus (M″) spectroscopy revealed the PT phase to have T_c ~480 and 440 °C for samples heat treated at ~550 and 700 °C, respectively. The conductivity of the PT phase and the dc conductivity of the glass heat treated at 700 °C were significantly higher than those of glasses heat treated at lower temperatures suggesting there is significant compositional differences between the glass heat treated at 700 °C compared to those treated at ≤650 °C.

Keywords Heat treatment · Glasses · Electron microscopy · Impedance spectroscopy

P. Sooksaen (✉) · I. M. Reaney · D. C. Sinclair
Department of Engineering Materials, University of Sheffield,
Sir Robert Hadfield Building, Mappin Street,
Sheffield S1 3JD, UK
e-mail: p_sooksaen@hotmail.com

1 Introduction

Glass-ceramics are polycrystalline solids prepared by controlled crystallization of glasses. They have been exploited in the electronics industry for some years due to advantages of preparing complex, large, fine-grained microstructures and pore-free bodies [1, 2]. Applications include materials used in substrates, dielectrics, pyroelectric and piezoelectric devices [2–4]. However, due to the limited number of published investigations the development in this area is slow and a better understanding of the relationships between crystallization, microstructure and electrical properties is still required. The properties of glass ceramics are mainly determined by the major crystalline phase but may deviate from the intrinsic properties due to the presence of a surrounding glass matrix or secondary phase(s). Studies relating to nucleation of high-permittivity ferroelectric crystals in glasses have been carried out since the early 1960s. Ferroelectric crystalline phases investigated include $SrTiO_3$ [5], $BaTiO_3$ [6, 7], $LiTaO_3$ [8], $LiNbO_3$ [8, 9], $NaNbO_3$ [10], $PbTiO_3$ (PT) [11–13] and $(Pb,Sr,Ba)Nb_2O_6$ [14]. Exploitation of pyroelectric, piezoelectric and/or electro-optic properties has been limited mainly due to difficulty in poling these materials.

This article investigates a glass composition of $39PbO–1BaO–25TiO_2–9.8Al_2O_3–1SiO_2–24.2B_2O_3$ (mol%) that has been shown to encourage low temperature densification of $PbTiO_3$, and prevent microcracking and pellet fracture when added as a sintering aid [15]. The composition is similar to that studied by Graaf et al. [12] and Shyu and Yang [13, 16] except the SiO_2 network has been replaced by B_2O_3. PT is the principal ferroelectric phase crystallized but the dielectric properties of any cerammed body are anticipated to be due a combination of PT and a low permittivity glass matrix or second phase. To separate out the electroactive elements in

the crystallized glasses, impedance spectroscopy [5] has been utilized in addition to more conventional characterization techniques such as X-ray diffraction (XRD) scanning and transmission electron microscopy (SEM and TEM). Impedance spectroscopy (IS) is a powerful tool for separating electroactive elements which contribute to the total electrical properties of a variety of materials, including electroceramics and glass-ceramics. Ferroelectric materials are particularly advantageous to study using IS as the capacitance associated with the bulk (or grain) response should be temperature dependent and exhibit a maximum at the ferro- to paraelectric phase transition (or Curie) temperature, T_c. This means a ferroelectric bulk phase can be readily distinguished from non-ferroelectric secondary phase(s) and/or residual glass, thus allowing variations in the electrical properties of the ferroelectric phase to be probed. To date, literature related to the study of ferroelectric glass-ceramics using IS has been limited.

Here the crystallization and dielectric properties of borate-based ferroelectric $PbTiO_3$ glass-ceramics are reported. Particular emphasis is given to analysis of the IS data using combined spectroscopic plots of the imaginary components of impedance ($-Z''$) and electric modulus (M''). The analysis shows how the electrical properties of the ferroelectric PT phase can be established in glass-ceramics and reveals the conductivity and T_c of the PT phase to be sensitive to the heat treatment temperature.

2 Experimental

2.1 Sample preparation

Glass was prepared via rough mixing of appropriate ratios of Pb_3O_4, $BaCO_3$, TiO_2, $Al(OH)_3$, B_2O_3 and Loch Aline (SiO_2) (all with purity ≥99%) and then transferring the batch to a platinum crucible for melting. Melting was carried out in an electric furnace for 2 h at 1200 °C, using a platinum stirrer after 1 h. Cold splatting was used to form clear glass instead of casting as a block to retard devitrification. The thin slab of glass was then cut into pieces ~10×10×1 mm and these were placed onto an alumina boat filled with alumina powder and cerammed for 4 h at temperatures between 520 and 700 °C with a heating and cooling rate of 5 °C/min. Above 700 °C, the samples distorted significantly presumably as a result of melting of the remaining glassy phase or one of the crystalline phases hence no higher temperature heat treatments were carried out.

2.2 Characterization

For X-ray diffraction (XRD) sample powders were analyzed on a Siemens D500 diffractrometer (Germany) with a scan speed of 1°/min and step interval 0.02° using Cu Kα radiation with a wavelength of 1.5406 Å, operated at 40 kV and 30 mA. Microstructures were studied using a JEOL JSM6400 SEM (Japan) and an EM420 TEM (Holland). Samples for SEM analysis were polished and etched with a 5 vol.% HF, 5 vol.% HNO_3, and 90 vol.% H_2O solution at room temperature for 60–70 s, followed by sputtering a gold conducting layer. Samples for TEM were thinned to electron transparency using a Gatan ion mill and then coated with a thin layer of carbon before analysis. Samples for electrical measurements were electroded with silver paste on the top and bottom faces and fired at 300 °C for 30 min (to remove organic binder from the silver paste) followed by 550 °C for 1 h. Electrical properties were studied by an Agilent 4294A, impedance analyser over a frequency range 10 Hz to 13 MHz.

2.3 Impedance spectroscopy background

Impedance spectroscopy (IS) measures the electrical impedance, Z, of samples as a function of frequency and usually over a wide temperature range. The contribution of different electro-active regions to the overall electrical behaviour can then be separated [17, 18]. Impedance data may be fitted to an equivalent circuit representative of the transport phenomena taking place in the system under investigation. Data can be analyzed using four interrelated formalisms; complex impedance, Z^*, admittance, Y^*, permittivity, ε^* and electric modulus, M^*, each with real and imaginary components e.g. $Z^* = Z' - jZ''$ and $M^* = M' + jM''$, where $j = \sqrt{-1}$. The interrelation can be expressed as $M^* = 1/\varepsilon^* = j\omega C_0 Z^* = j\omega C_0 (1/Y^*)$, where ω and C_0 are the angular frequency and capacitance of the empty cell, respectively [17, 18].

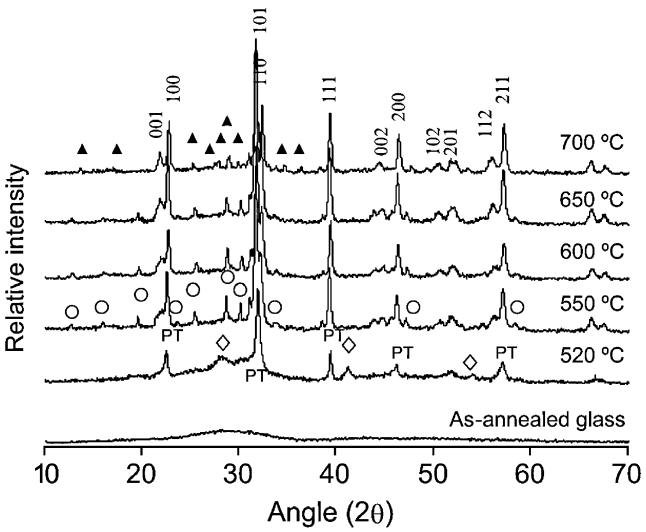

Fig. 1 XRD traces of glass heat treated from 520 to 700 °C for 4 h. Unknown transient phases (*diamond*), (*circle*) and $PbTi_3O_7$ (*triangle*)

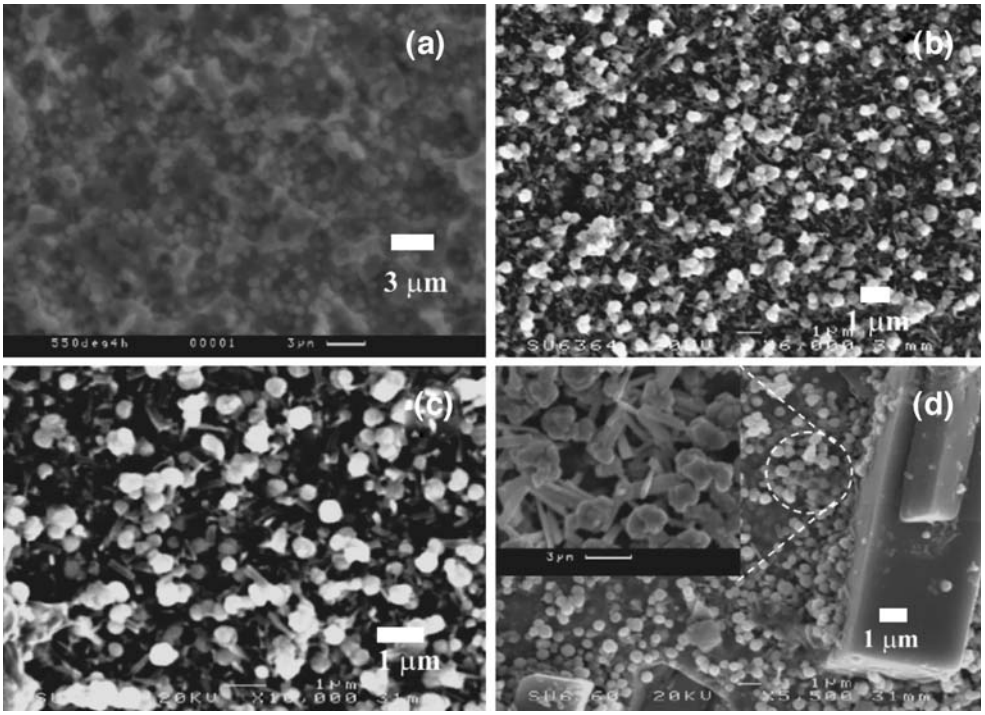

Fig. 2 SEM images of glass heat treated for 4 h at (**a**) 550, (**b**) 600, (**c**) 650 and (**d**) 700 °C. *Inset in* (**d**) is a higher magnification of the ringed region

Usually each electro-active region can be modeled to a first approximation on a resistor, R, and capacitor, C, connected in parallel. In the brickwork layer model for electroceramics these parallel RC elements are usually connected in series. Each RC element has a characteristic relaxation time or time constant, τ, which is given by the product of R and C, i.e. $\tau=RC$. The contribution of various elements to the electrical response and where they occur in the measured frequency range is determined by their relaxation times. Interface regions, such as grain boundaries are normally more resistive than the grains and also due to their small relative thickness compared to the grains have much higher capacitance values compared to the grain response. As a consequence, interfacial phenomena usually dominate the lower frequency range whereas the grain (or 'bulk' response) usually dominates at higher frequency.

For each RC element in an equivalent circuit, Z'' and M'' spectroscopic plots should contain a Debye peak. The Debye peaks in Z'' and M'' are expressed as $Z'' = R\left[(\omega RC)\Big/\left(1+(\omega RC)^2\right)\right]$ and $M'' = (\varepsilon_0/C)\left[(\omega RC)\Big/\left(1+(\omega RC)^2\right)\right]$ where ε_0 is the permittivity of free space and $\omega=2\pi f$ where f is the applied frequency in hertz. The peak maxima occur at the same frequency for a given element and the values of R and C can be easily calculated from the equations $Z''_{\max} = R/2$ and $M''_{\max} = \varepsilon_0/(2C)$. The relationship between R and C is $\omega_{\max}RC = 1$ where $\omega_{\max}$ is the frequency at the Debye peak maximum. It is noteworthy that Z'' spectra are dominated by RC elements with large R whereas RC elements with small C dominate M'' spectra. Thus, C_{grain} is usually much lower than C_{gb} and therefore

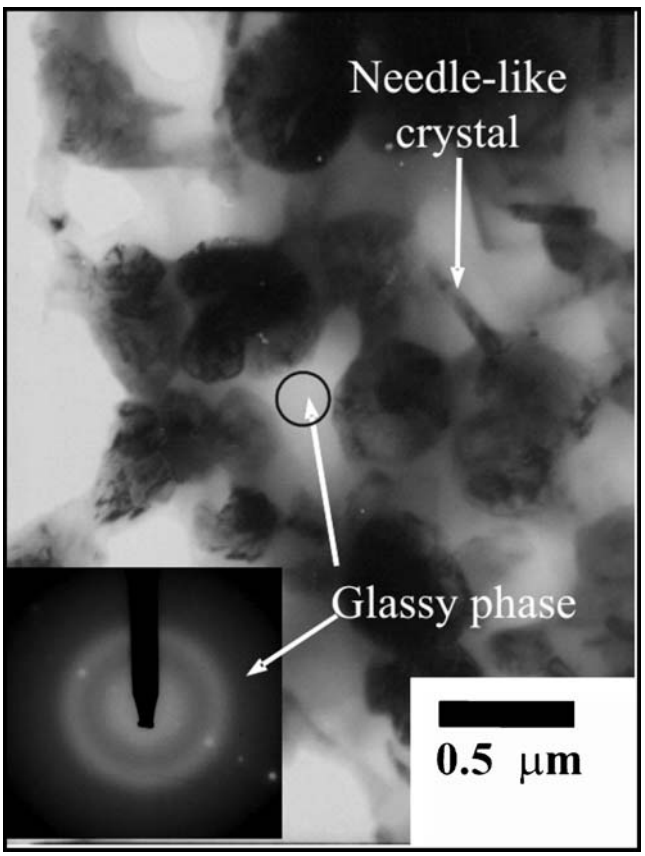

Fig. 3 Bright field TEM image of a sample heat treated at 650 °C. *Inset* is an amorphous halo diffraction pattern from the glassy phase

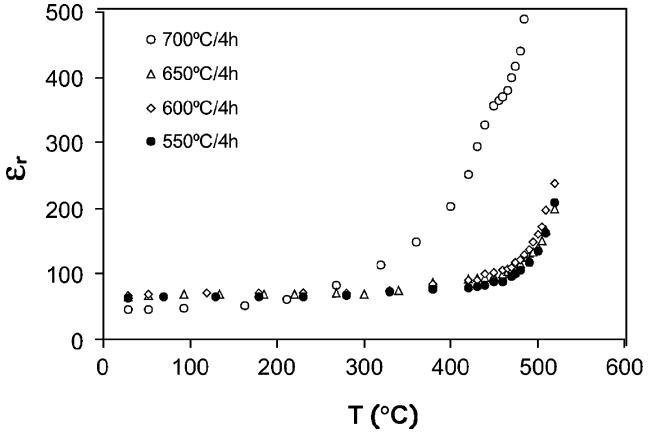

Fig. 4 ε_r vs temperature for different heat treated glass, measured at 100 kHz

M'' spectra tend to be dominated by the grain response. In most cases the Debye peaks are not ideal and this requires a constant phase element (CPE) to be connected in parallel with the R and C elements. However, in many cases the use of CPE and circuit modeling requires an in-depth study of the data. Our strategy here was to identify and characterize the bulk response from the samples as a function of heat treatment temperature as opposed to a detailed study of circuit fitting and analysis. To achieve our goal, hand fitting of the data was sufficient for this study. More details on IS analysis of electroceramics can be found from papers by Sinclair et al. [17, 19], Irvine et al. [18] and Fleig and Maier [20].

Conductivity, σ (where $\sigma=1/R$) associated with each electroactive element can also be obtained from IS data. The conductivity is usually plotted against reciprocal temperature (kelvin) in Arrhenius format and if a linear relation is obtained then the activation energy for conduction can be calculated from the slope using the following equation $\sigma = \sigma_0 \exp(-E_a/kT)$, where σ_0 is a pre-exponential factor, E_a is the activation energy for conduction (electron volt), k is the Boltzmann constant and T is the absolute temperature.

3 Results and discussion

3.1 XRD

Figure 1 shows XRD traces for samples heat treated from 520 to 700 °C for 4 h. After heat treatment at 520 °C tetragonal lead titanate (PT) starts to appear with a small c/a ratio ~1.01 along with an unidentified second phase, indicated by (⋄). As temperature increases, separation of the {hh0} and {h00} doublets increases commensurate with an increase in c/a, 1.031, 1.036, 1.041 and 1.044 for samples heat treated at 550, 600, 650 and 700 °C, respectively. At 550 °C, the unidentified second phase (♢) disappears but additional peaks are observed and are attributed to a third phase (○) which remains up to 650 °C. This third phase is also unidentified but disappears as a fourth phase (▲) evolves at 700 °C. This last phase to crystallise is possibly $PbTi_3O_7$ (JCPDS card No.45-533, monoclinic, space group P21).

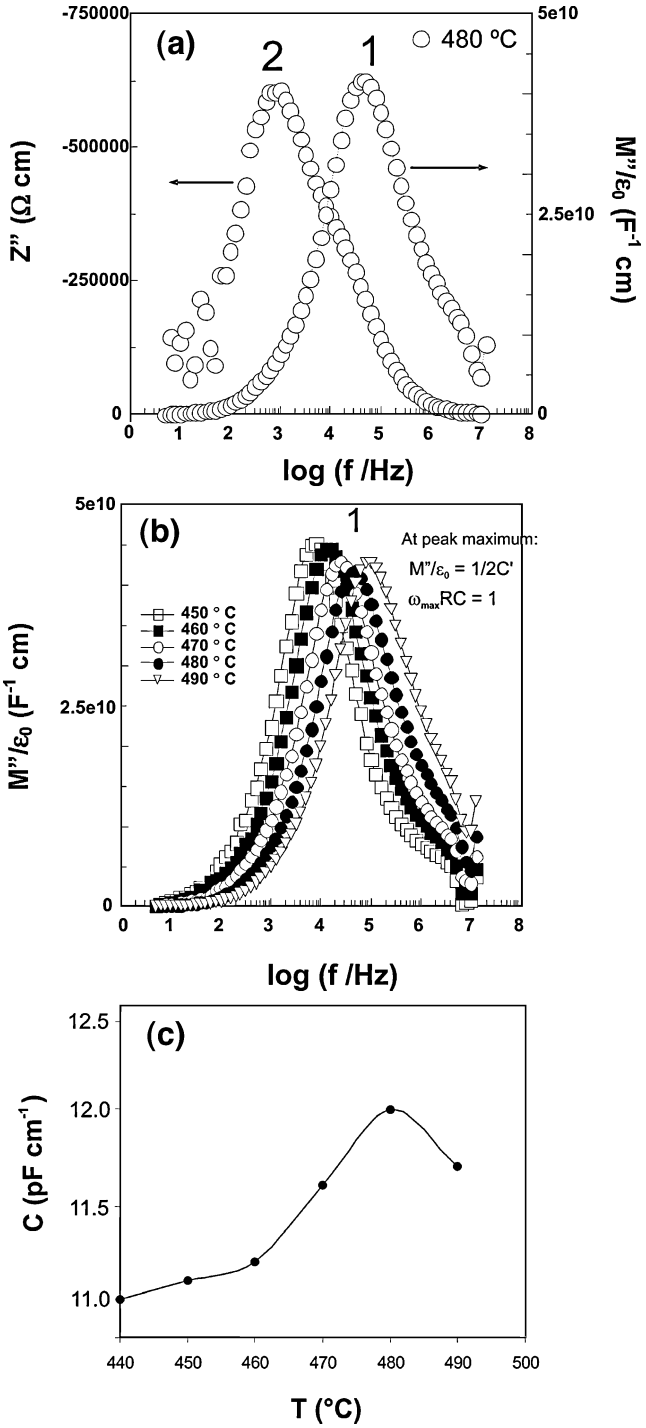

Fig. 5 (**a**) Combined Z'' and M'' spectroscopic plot at 480 °C for a sample heat treated at 550 °C/4 h, (**b**) M'' spectroscopic plots at various temperatures, and (**c**) extracted capacitance from peak 1 in (**b**) versus temperature

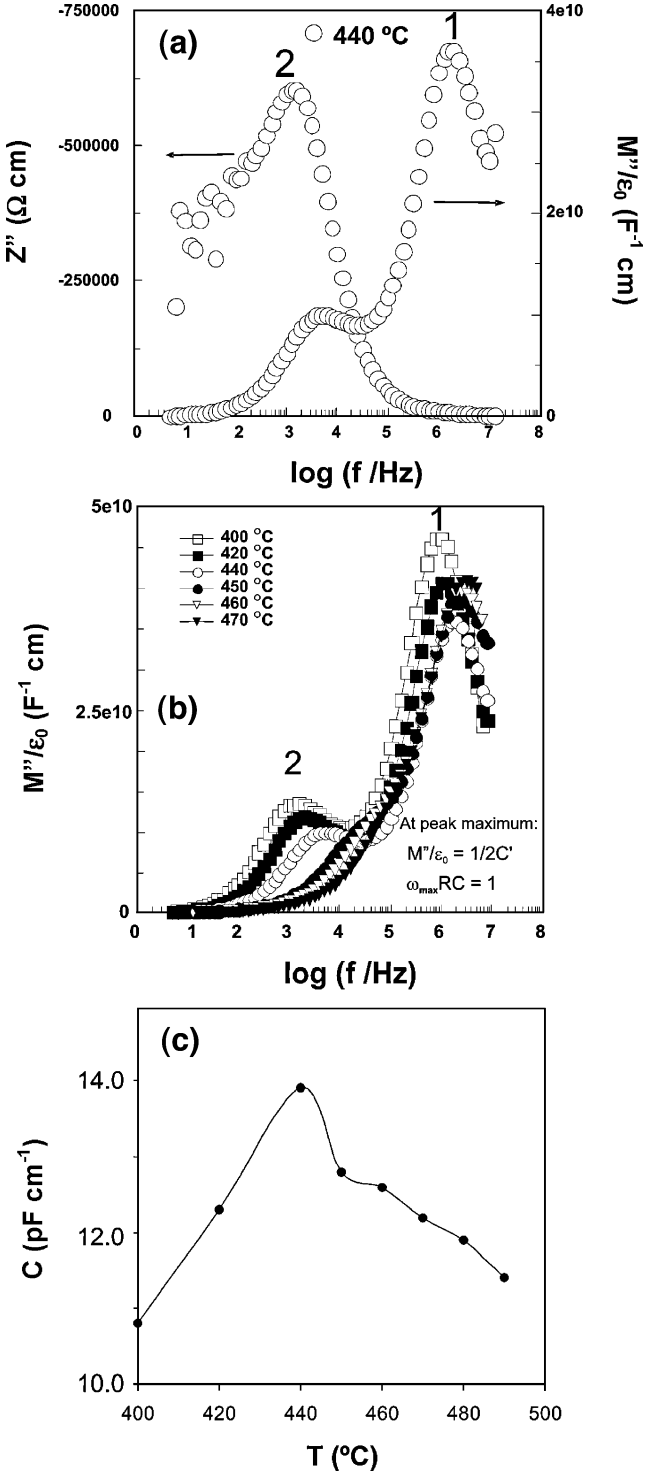

Fig. 6 (**a**) Combined Z'' and M'' spectroscopic plot at 440 °C for a sample heat treated at 700 °C/4 h, (**b**) M'' spectroscopic plots at various temperatures, and (**c**) extracted capacitance from peak 1 in (**b**) versus temperature

3.2 SEM and TEM analysis

Samples for SEM were selected from glass heat treated between 550 and 700 °C. Heat treatment at 550 °C (Fig. 2a) revealed small crystals (<0.3 μm) presumably originally dispersed within a glassy matrix which had been etched away. The size of these rounded crystals increased to ~0.5 μm at 700 °C. The rounded phase was consistent with PT according to energy dispersive X-ray spectroscopy. Figures 2(b),(c) and (d) are SEM images from samples heat treated at 600, 650 and 700 °C, respectively. The images show the rounded PT crystals and further needle-like crystals randomly dispersed, presumably within a glass matrix. These needle-like crystals can be correlated with the appearance of the unidentified phase (○) observed by XRD. In addition, at 700 °C, large laths are observed (approximately 50–100 μm) which are Ti-rich and are attributed to the $PbTi_3O_7$ phase in accordance with XRD data, Fig. 1. Figure 3 is a bright-field TEM image of a sample heat treated at 650 °C which reveals a substantial amount of amorphous glassy phase (inset Fig. 5) dispersed between the PT and needle-like crystals.

3.3 Electrical characterization

3.3.1 Fixed frequency measurements

Relative permittivity (ε_r) measured at 100 kHz versus temperature for different heat treated samples is shown in Fig. 4. The room temperature ε_r of samples heat treated between 550 and 650 °C show similar values between 63 and 67 and they follow the same trend with increasing temperature. For samples heat treated at 700 °C, the room temperature ε_r was 46. Above 400 °C, all samples show an increase in ε_r, however, only the 700 °C heat treated sample shows any evidence of a peak in permittivity near the expected T_c (~490 °C) of $PbTiO_3$. The sharp rise in permittivity above ~500 °C for all samples in Fig. 4 is

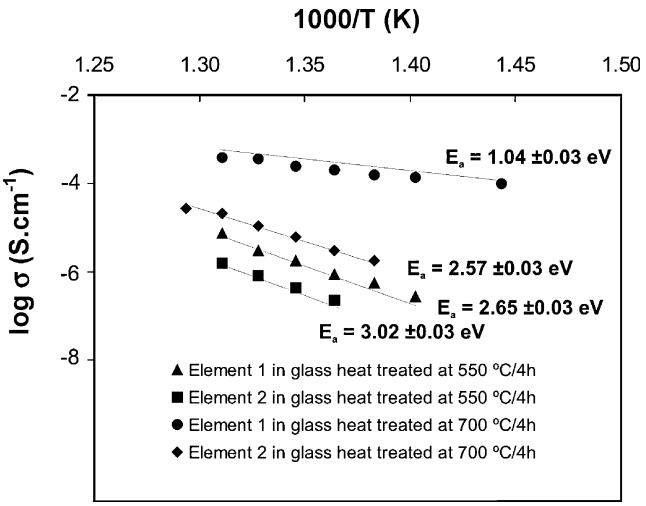

Fig. 7 Arrhenius plots of conductivity for elements 1 (PT) and 2 for glass treated at 550 and 700 °C/4 h. Please note element 1 and 2 values obtained from M'' and Z'' data, respectively

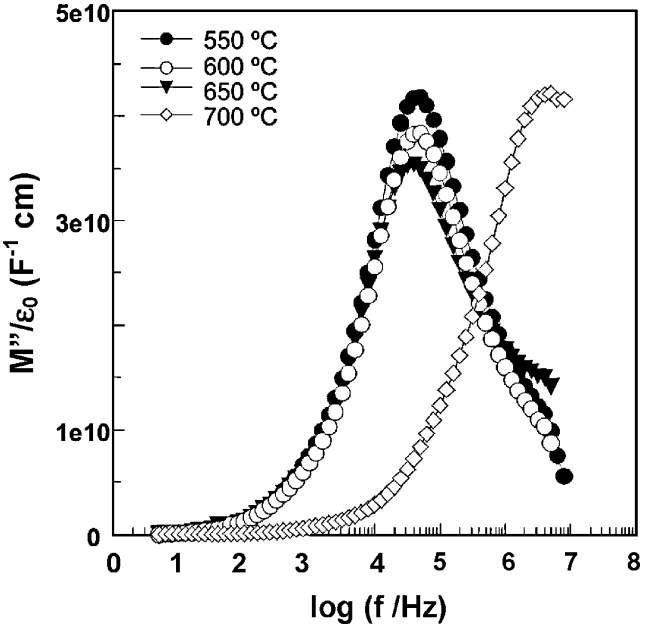

Fig. 8 M'' spectroscopic plots for different heat treated samples at 480 °C

attributed to increasing conductivity due to the elevated temperature.

3.3.2 Impedance spectroscopy (IS)

IS was carried out to investigate the contributions of each electroactive element to the electrical properties of the samples. Z^* plots at 500 °C (not shown) for all samples revealed evidence of two poorly resolved depressed arcs. Samples heat treated between 550 and 650 °C were much more resistive than samples heat treated at 700 °C. As samples heat treated between 550 and 650 °C show similar impedance responses, samples heat treated only at 550 and 700 °C are selected to discuss representative results in detail.

3.3.3 Analysis on glass heat treated at 550 °C

Impedance analysis of glass heat treated at 550 °C revealed two electroactive elements and could be modelled to a first approximation on an equivalent circuit based on two parallel RC elements connected in series. A combined Z'', M'' spectroscopic plot at 480 °C, Fig. 5(a), represents an example where one element (R_2C_2) has high resistance at low frequency and the other one (R_1C_1) has low capacitance at high frequency. Element 1 dominates the M'' spectrum and gives rise to the large M'' peak at higher frequency. In contrast, element 2 dominates the Z'' spectrum and gives rise to the large Z'' peak at lower frequency, Fig. 5(a). At 480 °C, the R and C values were estimated from the peak heights and using the relationship $\omega_{max}RC = 1$ as outline in the IS background section to be $R_1 \sim 32$ kΩ cm, $C_1 \sim 12.5$ pF cm^{-1}, $R_2 \sim 1.25$ MΩ cm and $C_2 \sim 127$ pF cm^{-1}.

Figure 5(b) shows M" spectroscopic plots at various temperatures. Analysis of element 1 shows the peak is responsible for the main PT phase as the M'' Debye peak height decreases to a minimum at ~480 °C and then increases in height above this temperature. This change is related to the phase transition temperature, T_c of PT which occurs in this temperature range (~490 °C for an undoped PT ceramic). The value of capacitance extracted from Fig. 5(b) at various temperatures is shown in Fig. 5(c) and the temperature dependence of capacitance confirms a phase transition characteristic of a ferroelectric phase. C_1 has magnitude of approximately 11–12 pF cm^{-1} which is consistent with a bulk ferroelectric response according to the brick layer model (BLM) for ceramics [17, 18]. In contrast, C_2 shows little temperature dependence and although the origin of element 2 is unknown, the magnitude of capacitance according to the BLM is consistent with that associated with either a minor (secondary phase), e.g. the residual transient phase (○) observed by XRD or residual glass, or with glass-crystal interfaces [5]. The temperature dependence of R_1 and R_2 will be discussed in the next section together with results obtained for glass heat treated at 700 °C.

3.3.4 Analysis on glass heat treated at 700 °C

Figure 6(a) shows a combined Z'', M'' spectroscopic plot at 440 °C. Again there appears to be two electroactive elements associated with this sample and the data can be modelled on an equivalent circuit of two parallel RC elements connected in series. Following the previous discussion the M'' peak at high frequency is associated with the PT phase (element 1). The M" peak height

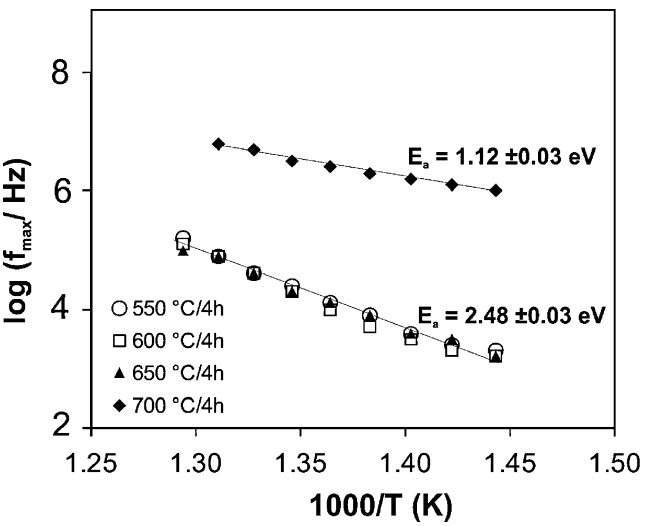

Fig. 9 log (f_{max}) vs 1,000/T for PT phase from various heat treated samples

decreases to a minimum at ~440 °C and subsequently increases again, Fig. 6(b). The variation of C_1 with temperature is shown in Fig. 6(c) and the behaviour is attributed to the phase transition temperature, T_c of the PT phase. The large peak in Z'' spectra at lower frequency is associated with a more resistive element, R_2 and is attributed to the presence of either minor/glassy phases or glass-crystal interfaces [5].

Arrhenius plots of conductivity for elements 1 (PT) and 2 for glass heat treated at 550 and 700 °C are shown in Fig. 7 where element 1 and 2 values were obtained from M" and Z" data, respectively. The data reveal the conductivity of the PT phase and element 2 to increase significantly for glass heat treated at 700 °C. In particular, the conductivity of the PT phase increases by at least two orders of magnitude for samples heat treated at 700 °C. The activation energy associated with conduction in the PT phase decreases from ~2.65 to ~1.04 eV on increasing the heat treatment to 700 °C, however the activation energy for conduction in element 2 shows a corresponding smaller decrease from ~3.02 to 2.57 eV.

3.3.5 Analysis of the PT phase from different heat treatments

M" spectroscopic plots at 480 °C for different heat treated samples are compared in Fig. 8. The peaks from these plots are responsible for the main PT phase (element 1) as mentioned earlier and it is clear that although the peak heights and therefore C for all four samples are similar, f_{max} for the sample heat treated at 700 °C occurs at significantly higher frequency compared to the other three samples, for which f_{max} is essentially constant. The characteristic time constant, τ ($=RC=1/\omega_{max}$) is a geometry independent parameter and therefore unlike the R and C values obtained from the analysis described above it does not depend on the volume fraction of the PT phase or the microstructure in the different heat treated glasses. Instead, τ (and therefore f_{max}) depends only on the intrinsic conductivity and permittivity of the PT phase and therefore any shift in f_{max} of the M'' spectra for element 1 can be attributed to some compositional change in the PT phase associated with heat treatment [21].

A plot of log (f_{max}) vs 1,000/T (where f_{max} is associated with the large peak in the M'' spectra) for various heat treated samples is shown in Fig. 9. For a fixed temperature, log (f_{max}) is similar for samples heat treated at 550, 600 and 650 °C whereas for those heat treated at 700 °C, f_{max} occurs at a significantly higher value. In addition, the activation energy associated with the bulk PT conduction is much lower (~1.12 eV) for the glass heat treated at 700 °C compared to that obtained (~2.48 eV) for those heat treated between 550 and 650 °C. The change in f_{max} (and therefore τ), activation energy for PT conduction and T_c observed for the glass heat treated at 700 °C implies the PT phase in this sample has a different composition compared to those heat treated at lower temperatures. The compositional change may have been caused by significant PbO/O_2 loss at elevated temperature leading to a 'more-lossy' PT phase with higher conductivity and lower activation energy of conduction.

4 Conclusions

A borate glass of $39PbO–1BaO–25TiO_2–9.8Al_2O_3–1SiO_2–24.2B_2O_3$ (mol%) crystallized on heat treatment ≥520 °C to form glass-ceramics with $PbTiO_3$ as the major phase. The crystal size and c/a ratio of PT were approximately the same for all heat treated samples. Crystallization between 520 and 650 °C induced the formation of two transient unidentified phases; the first at 520 °C followed by a second at 550 °C. At >650 °C, $PbTi_3O_7$ was present in addition to $PbTiO_3$. All samples contained significant quantities of residual glass phase.

The maximum in permittivity and T_c of PT was not observed from fixed frequency capacitance measurements for samples heat treated below 700 °C, however IS revealed the electrical properties of the PT phase could be probed using electric modulus spectroscopy. Glass heat treated at 700 °C is more electrically conducting than those heat treated at lower temperatures and T_c is also lowered from ~480 to 440 °C. These results indicate significant compositional changes occur in the PT phase on heating these glasses at 700 °C. This information is not readily available from fixed frequency capacitance measurements and demonstrates the usefulness of IS to probe variations in composition and electrical properties of a ferroelectric phase in electrically heterogeneous glass ceramics.

References

1. B. Aitken, G. Beall, in *Glass-Ceramics, in Materials Science and Technology: A Comprehensive Treatment. Structure and properties of ceramics*, ed. by P.H. R.W. Cahn, E.J. Kramer (Wiley, New York, 1997), pp. 266–294
2. A.Halliyal, A.S. Bhalla, R.E. Newnham, L.E. Cross, in *Glass-ceramics for piezoelectric and pyroelectric devices, in Glasses and glass-ceramics*, ed. by M.H. Lewis, (Chapman and Hall, University Press Cambridge, London, 1989)
3. G.E. Rindone, in *Proceedings of the Symposium on Nucleation and Crystalllization in Glasses and Melts*, American Ceramic Society, Columbus, 1962.
4. G.J. Gardopee, R.E. Newnham, A. Halliyal, A.S. Bhalla, Pyroelectric glass-ceramics. Appl. Phys. Lett. **36**(10), 817–818 (1980)
5. O.P. Thakur, D. Kumar, O. Parkash, L. Pandey, Electrical characterization of $SrTiO_3$ borosilicate glass ceramics system with

bismuth oxide addition using impedance spectroscopy. Mat. Chem. and Phys. **78**, 751–759 (2003)
6. K. Yao, L. Zhang, Preparation and structure of $BaTiO_3$ ferroelectric glass-ceramics. Chin. Sci. Bull. **40**(8), 694–698 (1995)
7. A. Herczog, Microcrystalline $BaTiO_3$ by crystallization from glass. J. Am. Ceram. Soc. **47**(3), 107–115 (1964)
8. M. Cable, J.M. Parker, High performance glasses. (Chapman and Hall, New York, 1992)
9. A.M. Glass, M.E. Lines, K. Nassau, J.W. Shiever, Anomalous dielectric behavior and reversible pyroelectricity in a roller-quenched $LiNbO_3$ and $LiTaO_3$ glass. Appl. Phys. Lett. **31**(4), 249–251 (1977)
10. M.M. Layton, A. Herzog, Nucleation and crystallization of $NaNbO_3$ from glasses in the Na_2O–Nb_2O_5–SiO_2 system. J. Am. Ceram. Soc. **50**(7), (1967)
11. D.G. Grossman, .J.O. Isard, Lead titanate glass-ceramics. J. Am. Ceram. Soc. **52**(4), 230 (1969)
12. M.A.C.G.V.d Graaf, A.J. Burggraaf, J.C. Lodder, Microstructure development and crystallization kinetics of $PbTiO_3$ from PbO–TiO_2–$Al2O_3$–SiO_2 glass. Glass Technol. **15**(16), 143–147 (1974)
13. J.J. Shyu, Y.S. Yang, Crystallization of a PbO–BaO–TiO_2–Al_2O_3–SiO_2 glass. J. Am. Ceram. Soc. **78**(6), 1463–1468 (1995)
14. M.J. Reece, C.A. Worrell, G.J. Hill, R. Morrell, Microstructures and dielectric properties of ferroelectric glass-ceramics. J. Am. Ceram. Soc. **79**(1), 17–26 (1996)
15. P. Sooksaen, I.M. Reaney, D.C. Sinclair, Engineered sintering aids for PbO-based electroceramics. Journal of Electroceramics **18**, 77 (2007)
16. J.J. Shyu, Y.S. Yang, Crystallization and properties of a perovskite glass-ceramic. J. Materials Sci. **31**, 4859–4863 (1996)
17. A.R. West, D.C. Sinclair, N. Hirose, Characterization of electrical materials, especially ferroelectrics by impedance spectroscopy. J. Electroceramics. **1**(1), 65–71 (1997)
18. J.T.S. Irvine, D.C. Sinclair, A.R. West, Electroceramics: Characterization by impedance spectroscopy. Adv. Mater. **2**(3), 132–138 (1990)
19. D.C. Sinclair, A.R. West, Impedance and modulus spectroscopy of semiconducting barium titanate showing positive temperature coefficient of resistance. J. Appl. Phys. **66**, 3850 (1989)
20. J. Fleig, J. Maier, The impedance of ceramics with highly resistive grain boundaries: Validity and limits of the brick layer model. J. Eur. Ceram. Soc. **19**, 693–696 (1999)
21. F.D. Morrison, D.C. Sinclair, A.R. West, Characterization of lanthanum-doped barium titanate ceramics using impedance spectroscopy. J. Am. Ceram. Soc. **84**(3), 531–538 (2001)